

Possibility of observing MSSM charged Higgs in association with a W boson at LHC

M. Hashemi

School of Particles and Accelerators, Institute for Research in Fundamental Sciences (IPM), P.O. Box 19395-5746, Tehran, Iran

Possibility of observing associated production of charged Higgs and W boson in the framework of MSSM at LHC is studied. Both leptonic and hadronic decays of W boson are studied while the charged Higgs boson is considered to decay to a τ lepton and a neutrino. Therefore two search categories are defined based on the leptonic and hadronic final states, i.e. $\ell \tau + E_T^{miss}$ and $jj \tau + E_T^{miss}$ where $\ell = e$ or μ and j is a light jet from W decay. The discovery chance of the two categories is evaluated at an integrated luminosity of 300 fb^{-1} at LHC. It is shown that both leptonic and hadronic final states have the chance of discovery at high $\tan\beta$. Finally 5σ and 3σ contours are provided for both search categories.

I. INTRODUCTION

The Standard Model of particle physics has obtained a magnificent success through the experimental precision tests in the last years. Despite its success, the main part of the theory, i.e. the Higgs mechanism and the question of mass spectrum has remained unexplored and out of reach by the recent experiments. One of the main goals of upcoming experiments especially the Large Hadron Collider experiment (LHC) at CERN is to search for the Higgs boson as the predicted particle through the Higgs mechanism. While prediction of a single Higgs boson in the SM appears to be incomplete and reveals theoretical problems such as the Higgs boson mass divergence when including radiative corrections, theoretical models beyond the SM appear to be attractive candidate solutions to the SM Higgs sector problems. The supersymmetric extensions to the SM are one of these models which not only provide elegant solutions to the Higgs boson mass divergence by introducing supersymmetric partners for SM particles but also provide approaches for other issues such as the gauge couplings unification Ref. [1]. The family of two Higgs doublet models (2HDM) which introduce two Higgs doublets instead of a single scalar Higgs particle are of special interest among the supersymmetric models. The minimal supersymmetric extension to the SM, the so called MSSM, appears as a simple, reliable and minimal model belonging to the 2HDM family which predicts five physical Higgs bosons two of which are charged. While the neutral Higgs bosons of MSSM might be hard to distinguish from neutral Higgs boson of the SM, the observation of a charged Higgs is a crucial signature of theories beyond the SM. This is an enough reason that this particle has attracted special attention in the last years in different High Energy Physics experiments and will certainly be probed at the LHC experiment at CERN.

A large number of searches have been carried out in CMS and ATLAS collaborations of LHC. The overall result is promising and predicts a possible discovery of charged Higgs boson at integrated luminosities of the order of 30 fb^{-1} (Refs. [2], [3], [4], [5]). There are also early data searches such as Ref. [6]. Two search areas based on the charged Higgs boson mass have been considered in the above analyses. The light charged Higgs search area which covers charged Higgs masses below the top quark mass uses $t\bar{t}$ production as the signal process with the following decay chain $t\bar{t} \rightarrow H^\pm W^\mp b\bar{b}$. The charged Higgs boson is considered to decay to a τ lepton which decays hadronically. The W boson is forced to decay to e or μ (the leptonic final state) or light jets (hadronic final state). The heavy charged Higgs search area covers all charged Higgs masses above the top quark mass and uses $gg \rightarrow t\bar{t}H^\pm$ and $gb \rightarrow tH^\pm$ with a combination procedure described in Refs. [7] and [8]. Both decay channels $H^\pm \rightarrow \tau^\pm \nu_\tau$ and $H^\pm \rightarrow t\bar{b}$ are considered for heavy charged Higgs search, however, the latter does not lead to a promising discovery chance leaving the attention to be paid to the tauonic decay of the charged Higgs as the main decay channel throughout the parameter space.

In this paper the associated production of charged Higgs and a W boson as a complementary search channel to the current analyses is studied. There has been a previous analysis of this process reported in Ref. [9]. The current analysis aims at two main purposes as complementary to the previous analysis: first including a reasonable set of main background processes in the analysis i.e. $t\bar{t}$, WW and W +jets and estimating their contribution, and second extending the search to the leptonic final state which involves leptonic decay of W boson (i.e. $W \rightarrow \ell \nu$ where $\ell = e$ or μ). The analysis starts with heavy charged Higgs which is studied in two categories of leptonic and hadronic final states. Then light charged Higgs signal is analyzed and two production processes, i.e. $H^\pm W^\mp$ and $t\bar{t} \rightarrow H^\pm W^\mp b\bar{b}$ are compared in both final states. A set of simulation packages is used for the analysis and a set of selection cuts is applied on the main distinguishing kinematic variables to increase the signal to background ratio. Finally the signal statistical significance is evaluated as a function of the charged Higgs mass and $\tan\beta$ and 5σ and 3σ contours are plotted.

Process	Signal		Background		
	$H^\pm W^\mp$ $m_{(H^\pm)} = 150 \text{ GeV}$	$H^\pm W^\mp$ $m_{(H^\pm)} = 175 \text{ GeV}$	$W^+ W^-$	$t\bar{t}$	$W+\text{jets}$
Cross Section	1.47 pb	1.18 pb	$115.5 \pm 0.4 \text{ pb}$	$878.7 \pm 0.5 \text{ pb}$	$187.1 \pm 0.1 \text{ nb}$

TABLE I: Signal and Background cross sections calculated using MCFM package.

II. SIGNAL AND BACKGROUND PROCESSES

The signal process is $b\bar{b} \rightarrow H^\pm W^\mp$ followed by the decay $H^\pm \rightarrow \tau^\pm \nu_\tau$. The reason for using only $b\bar{b}$ initiated process is that the dominant contribution comes from $b\bar{b}$ and the relative contribution of gg process becomes small and negligible ($O(10^{-2})$) at high $\tan\beta$. This argument is in accord with Refs. [11] and [12]. Depending on the W boson decay two search categories are defined as the leptonic final state i.e. $W^\pm \rightarrow \ell\nu$ where $\ell = e$ or μ and the hadronic final state i.e. $W^\pm \rightarrow jj$ where j is a light quark initiating a jet. Therefore the two signal processes under study are $b\bar{b} \rightarrow H^\pm W^\mp \rightarrow \tau^\pm \nu_\tau \ell\nu$ and $b\bar{b} \rightarrow H^\pm W^\mp \rightarrow \tau^\pm \nu_\tau jj$.

The background processes which are studied in this analysis are $t\bar{t}$, WW and $W+\text{jets}$. In the search for the leptonic final state, the $t\bar{t}$ process is forced to produce the following final states $t\bar{t} \rightarrow WbWb \rightarrow \ell\tau bb E_T^{miss}$ or $\ell jj bb E_T^{miss}$. In the same search the following final state for WW process is considered: $WW \rightarrow \ell\tau E_T^{miss}$ or $\ell jj E_T^{miss}$. The $W+\text{jets}$ is used with $W \rightarrow \ell\nu$. All these processes are included to account for non-identified jets which escape the reconstruction and also the τ jet fake rate which comes from light quark jets present in the event which pass the τ identification algorithm.

Subsequently the hadronic final state search is performed with forcing $t\bar{t}$ events to decay to the following final states $t\bar{t} \rightarrow WbWb \rightarrow \tau jj bb E_T^{miss}$ or $\tau\tau bb E_T^{miss}$ or $jj jj bb$ while WW process is forced to decay to $WW \rightarrow \tau jj E_T^{miss}$ or $\tau\tau E_T^{miss}$ or $jj jj$. In the $W+\text{jets}$ simulation the W boson can decay as $W \rightarrow \tau E_T^{miss}$ or $W \rightarrow jj$.

III. EVENT SIMULATION

Signal events are simulated using PYBBWH code Ref. [13] which is linked to PYTHIA 6.4.21 Ref. [14]. The τ leptons polarization and decays are controlled by the TAUOLA package (Refs. [15], [16] and [17]) which is linked to PYTHIA. Throughout the analysis τ leptons are identified through their hadronic decays which results in a narrow τ jet which will be described in detail later in the next sections. The analysis is based on parton showering and hadronization. The jet reconstruction is performed using PYTHIA built-in jet reconstruction tool, PYCELL, with a cone size of 0.5. Only jets within the pseudorapidity range of $|\eta| < 3.0$ are reconstructed. The parton distribution function used in the analysis is MRST 2004 NNLO which is used by linking LHAPDF 5.8.1 Ref. [18] to the PYTHIA event generator. For the signal simulation the $m_{h^0} - \text{max}$ scenario is used with the following parameters: $M_2 = 200 \text{ GeV}$, $M_{\tilde{g}} = 800 \text{ GeV}$, $\mu = 200 \text{ GeV}$ and $M_{SUSY} = 1 \text{ TeV}$.

IV. SIGNAL AND BACKGROUND CROSS SECTIONS

The signal cross section is calculated by the joint PYTHIA+PYBBWH package using the MRST 2004 NNLO PDF set. The background cross sections are calculated using MCFM 5.7 Ref. [19] at next to leading order with the same PDF set as above. Table I lists the total cross sections of different processes used in the analysis. The branching ratios used in the analysis are $\text{BR}(t \rightarrow W^\pm b) = 0.77$, $\text{BR}(t \rightarrow H^\pm b) = 0.23$ for $m_{(H^\pm)} = 150 \text{ GeV}$, $\text{BR}(H^\pm \rightarrow \tau\nu) = 0.987$ which is almost constant for the mass range $m_{(H^\pm)} < 175 \text{ GeV}$. The W boson is considered to decay according to the following branching ratios $\text{BR}(W^\pm \rightarrow \ell\nu) = 0.106$ and $\text{BR}(W^\pm \rightarrow jj) = 0.68$ which are taken from Particle Data Group (PDG) at Ref. [20]. The branching ratios of charged Higgs decays are calculated using HDECAY 3.51 Ref. [21]. The branching ratio of top quark decay to charged Higgs is taken from PYTHIA.

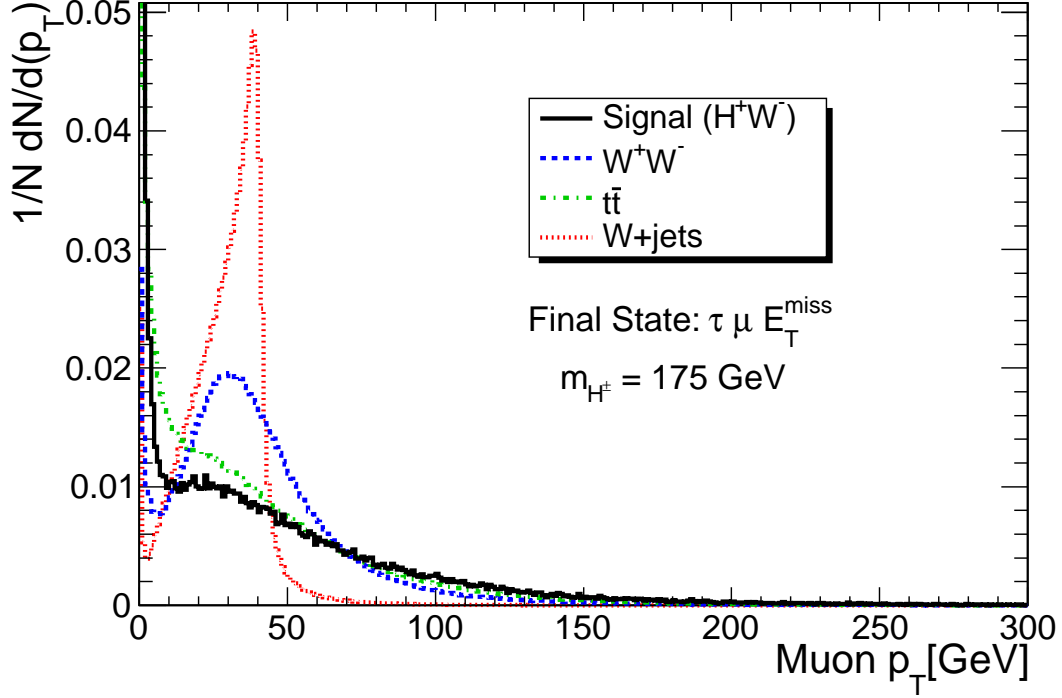


FIG. 1: Transverse momentum distribution of muons in signal and background events in the $\tau\mu E_T^{\text{miss}}$ final state .

V. EVENT ANALYSIS AND SIGNAL SEARCH

In this section the event analysis is described in detail. The search is divided into two regions of low mass and high mass charged Higgs with the separating point set to $m_{(H^\pm)} = m_{\text{top}} - m_{\text{bottom}}$ which is the end point beyond which the production process $t\bar{t}$ is pure SM process and no on-shell $t \rightarrow H^\pm b$ decay is allowed.

A. Heavy Charged Higgs Search, Leptonic Final State

In the following, a heavy charged Higgs with a mass of 175 GeV is analyzed in leptonic final state. This is a point in parameter space close to the defined border at which the on-shell $t\bar{t} \rightarrow H^\pm W^\mp b\bar{b}$ process dies and the charged Higgs may only be produced by $gg \rightarrow t\bar{b}H^- + gb \rightarrow tH^-$ or $H^\pm W^\mp$. The aim of this work is to solely estimate the amount of excess one may observe over SM processes if a search is designed for $H^\pm W^\mp$ events. The set of selection cuts is described below. An event must contain all the following objects to be selected:

- One muon satisfying Eq. 1:

$$p_T^\mu > 50 \text{ GeV}, \quad |\eta| < 2.5. \quad (1)$$

where η is pseudorapidity defined as

$$\eta \equiv -\log \left[\tan \frac{\theta}{2} \right]$$

in which θ is the angle between the momentum and the beam axis. The adopted threshold in Eq. 1 has been inspired by Fig. 1.

- One reconstructed jet satisfying Eq. 2:

$$E_T^{\text{jet}} > 50 \text{ GeV}, \quad |\eta| < 2.5. \quad (2)$$

This cut is also adopted in accord with Fig. 2. To reject the contribution of non-isolated muons which come mainly

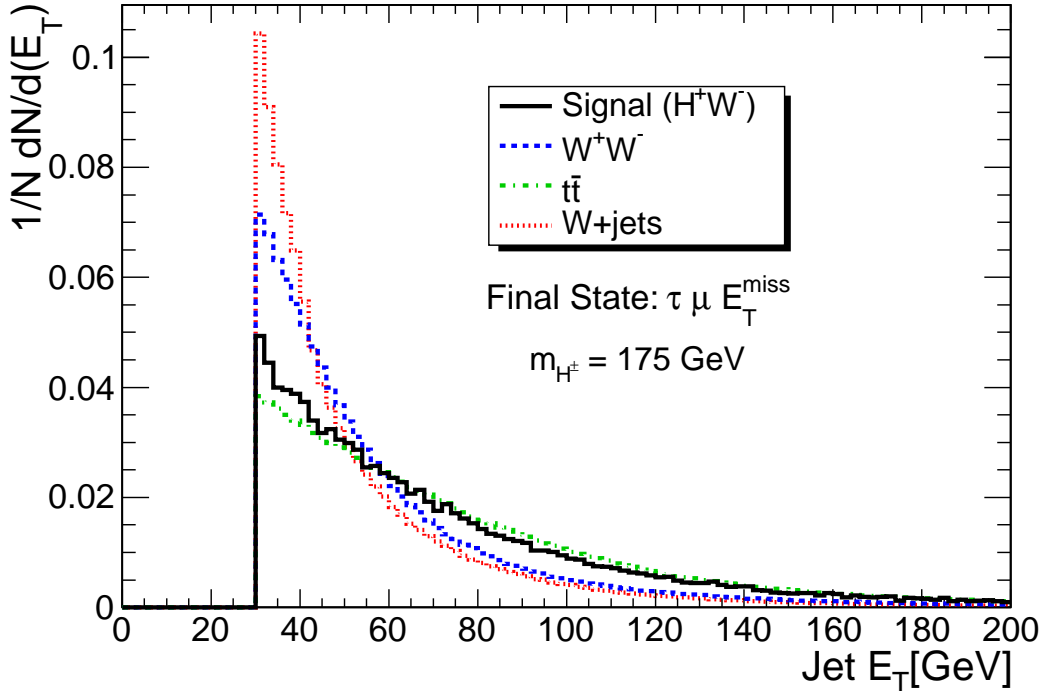


FIG. 2: Transverse energy distribution of reconstructed jets in signal and background events in the $\tau\mu E_T^{\text{miss}}$ final state. All jets with $E_T < 30$ GeV are thrown away in the event as a general cut-off on the jet transverse energy. This is adopted usually in full simulation analyses to reject contribution of soft jets from pile-up events and also avoid reliability issues related to performance of the jet reconstruction algorithm at low transverse energies.

from heavy meson decays, the selected jet and muons with $p_T > 20$ GeV should be separated enough with the following requirement:

$$\Delta R_{(\text{jet}, \mu)} > 0.4. \quad (3)$$

Here ΔR is defined as $\Delta R = \sqrt{(\Delta\eta)^2 + (\Delta\phi)^2}$.

The τ identification algorithm is then applied on the reconstructed jet in the event. A jet is accepted if it passes all the requirements of τ -id. Although in a full simulation analysis there may be sophisticated requirements for τ jets, here the basic requirements are applied. These requirements identify τ jets with a reasonable purity. However the τ fake rate (contribution of non- τ jets which pass the τ -id algorithm) may be higher than in a real analysis with full τ -id cuts. This fact arises hopes for better results with less background contamination in the signal sample. Verification of this issue is beyond the scope of this analysis which is providing prospects of the observability of this channel at the LHC and motivation of performing this analysis by LHC experiments, CMS and ATLAS.

The τ -id which is used in the analysis is similar to the one used by the CMS collaboration Ref. [22]. In this analysis all decays of τ leptons are turned on but the search is only based on the hadronic decays which in total account for $\sim 65\%$ of the total decay width of the τ lepton. The τ lepton in its hadronic decay produces predominantly one or three charged pions. Due to the low charged track multiplicity in the final state, the charged tracks (pions) in the τ hadronic decay acquire relatively a higher transverse momentum compared to tracks of light quark jets. To study this effect, a jet-track matching cone of $\Delta R = 0.1$ is considered around the jet axis. The hardest charged track in the matching cone is considered as the charged pion from the τ lepton decay. Figure 3 shows distribution of the leading track transverse momentum in the matching cone around the jet. To exploit this feature a transverse momentum threshold is applied as the following:

$$p_T^{\text{leading track}} > 20 \text{ GeV}. \quad (4)$$

Since τ jets consist of few charged tracks, they are considered as isolated jets. To check if a τ jet is isolated an isolation cone and a signal cone is defined respectively with a cone size of $\Delta R < 0.4$ and $\Delta R < 0.07$ around the

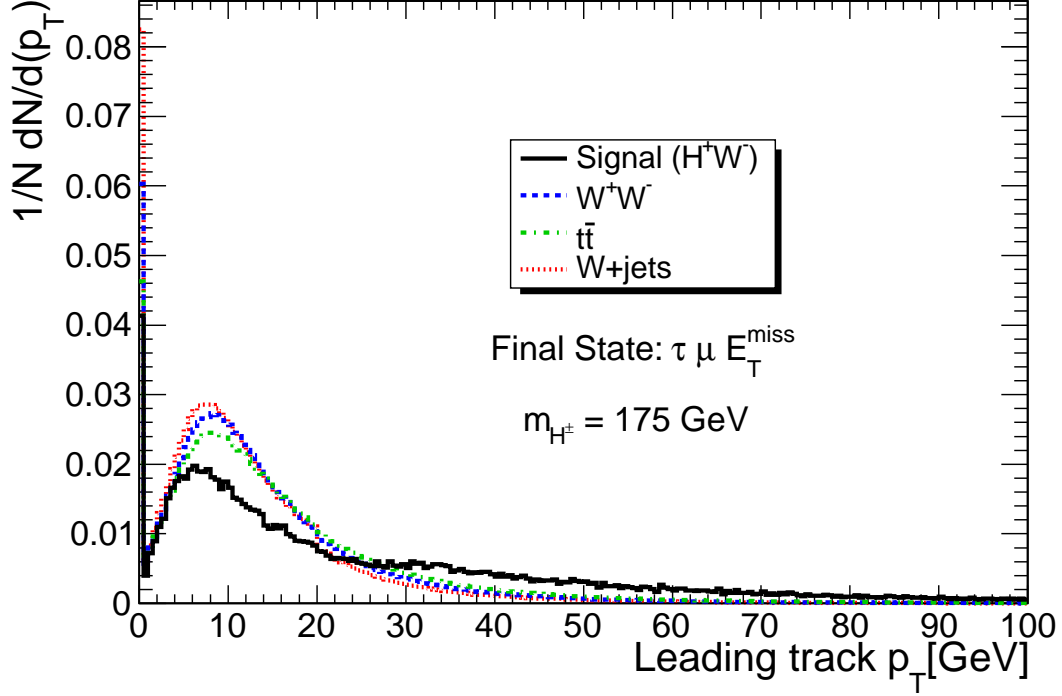


FIG. 3: Transverse momentum distribution of the leading track in the τ jet cone.

leading track. The isolation is applied by requiring no charged track with $p_T > 1$ GeV to be in the isolation annulus defined as $0.07 < \Delta R < 0.4$.

The low charged track multiplicity in the τ jets also implies that the leading track in the jet cone carries a larger fraction of the τ jet energy compared to quark jets in background events. This effect can be verified by plotting distribution of the leading track p_T divided by the τ jet energy as shown in Fig. 4. In order to keep the signal statistics at a reasonable amount, a soft cut on this quantity is applied as the following:

$$R = \text{leading track } p_T / E_{\tau\text{-jet}} > 0.2 . \quad (5)$$

The number of charged tracks in the τ jet is also evaluated by a search in the signal cone and the following requirement is applied:

$$\text{Number of signal tracks} = 1 \text{ or } 3 . \quad (6)$$

Figure 5 shows distribution of the number of signal tracks in signal events before applying the cut. As seen from Fig. 5, τ jets have undergone 1- or 3-prong decays predominantly. The azimuthal angle between the muons and τ leptons is also investigated as shown in Fig. 6. As is observed from Fig. 6, background events tend to produce a harder back-to-back topology, however, in order to keep the signal statistics, no cut on this kinematic variable is applied. In the next step the τ lepton charge is calculated as the sum of charges of tracks in the signal cone. Since muons and τ leptons in signal events are produced with opposite charges, the following requirement is applied:

$$\text{Muon charge} + \tau \text{ jet charge} = 0 . \quad (7)$$

• A reasonable amount of missing transverse energy should be left in the event. This is because of spin considerations and the fact that in $H^\pm W^\mp$ events, neutrinos tend to fly collinearly which is the result of charged Higgs boson being a spinless particle. The transverse missing energy distribution is studied as shown in Fig. 7. As seen from Fig 7, the main backgrounds are all produced with a low E_T^{miss} compared to signal events. The following requirement is therefore applied on E_T^{miss} :

$$E_T^{\text{miss}} > 50 \text{ GeV} . \quad (8)$$

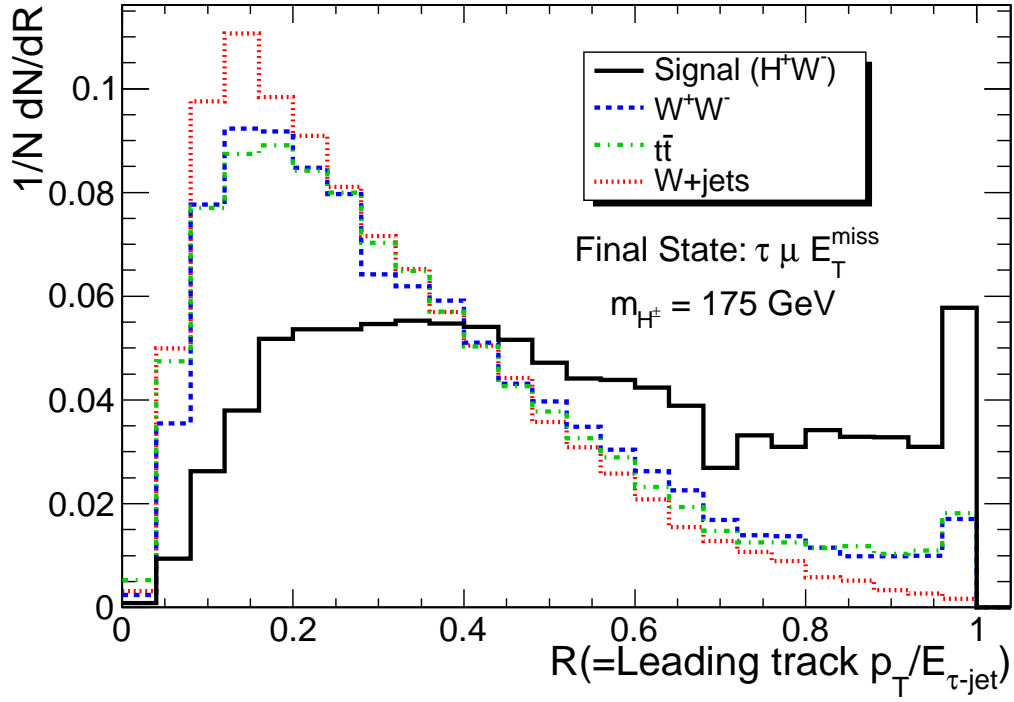


FIG. 4: Distribution of the leading track p_T divided by the τ jet energy.

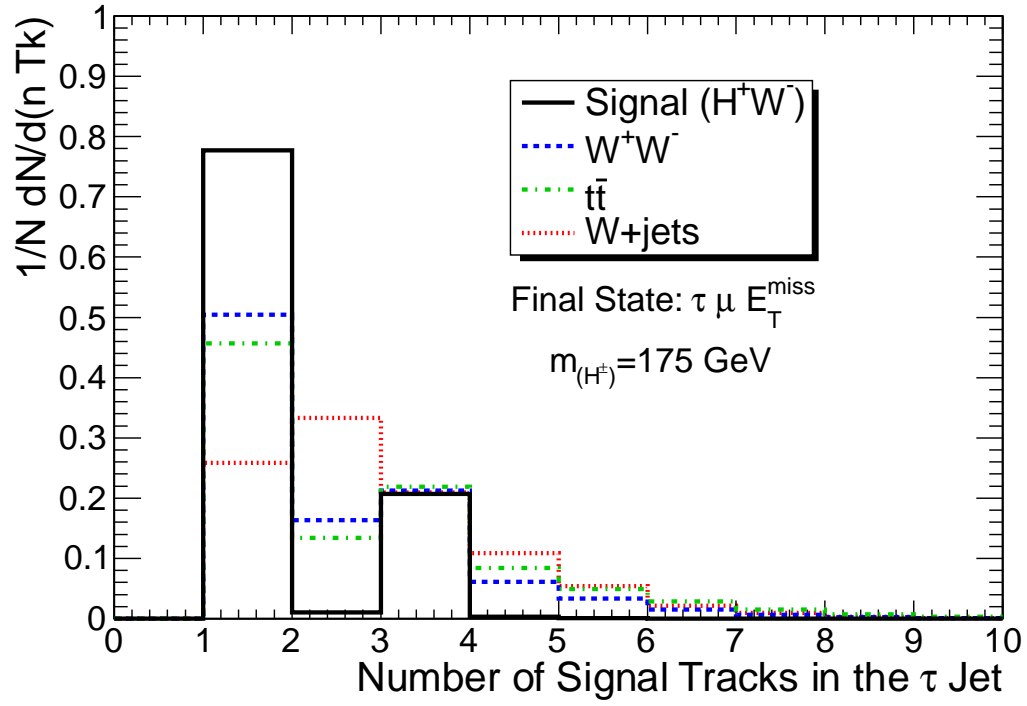


FIG. 5: Number of tracks in the signal cone around the leading track of the τ jet.

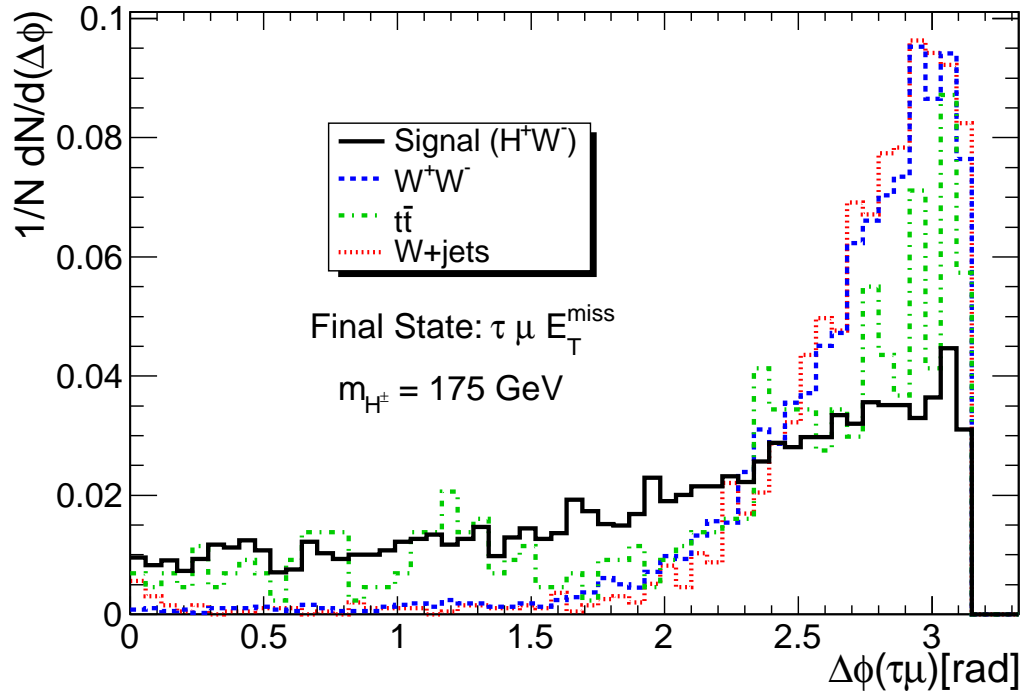


FIG. 6: The azimuthal angle between the muon and the τ jet candidate in the $\tau\mu E_T^{\text{miss}}$ final state.

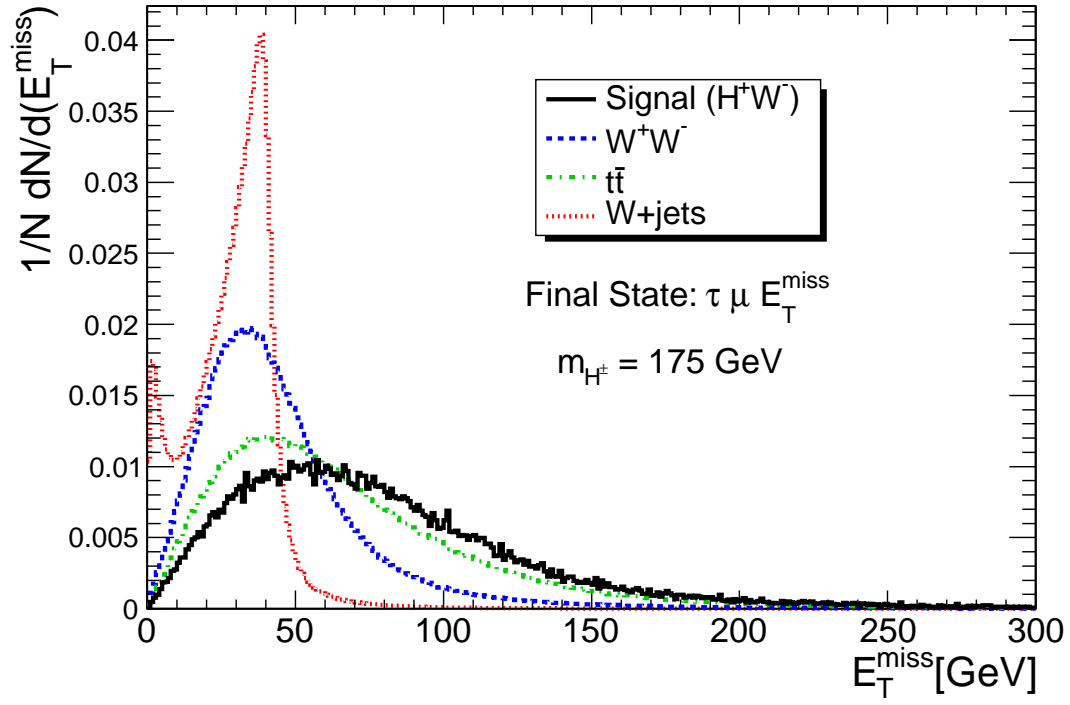


FIG. 7: Missing transverse energy distribution in signal and background events in the $\tau\mu E_T^{\text{miss}}$ final state.

Process	$H^\pm W^\mp$	$W^+ W^-$	$t\bar{t}$	W+jets
Total cross section [pb]	1.18	115.5	879	187100
Number of events at 30 fb^{-1}	3695	577577	4394086	5.9×10^8
N Muons = 1	1725(46.7%)	141662(24.5%)	1.73e+06(39.3%)	1.34e+07(2.3%)
N Jets = 1	762(44.2%)	62159(43.9%)	120121(6.9%)	6.2e+06(46.6%)
leading track $p_T > 20\text{ GeV}$	431(56.5%)	19327(31.1%)	35557(29.6%)	1.5e+06(24.9%)
Isolation	352(81.7%)	3676(19%)	3247(9.1%)	133281(8.6%)
R > 0.2	308(87.4%)	2617(71.2%)	2223(68.5%)	86887(65.2%)
1- or 3-prong decay	303(98.4%)	2177(83.2%)	1916(86.2%)	38389(44.2%)
Opposite charge	302(99.8%)	2146(98.6%)	1885(98.4%)	35577(92.6742%)
$E_T^{miss} > 50\text{ GeV}$	215(71.2%)	776(36.1%)	1112(59%)	3737(10.5%)
Total efficiency	5.83%	0.13%	0.025%	$6.3 \times 10^{-4}\%$
Expected events at 30 fb^{-1}	215	776	1112	3737

TABLE II: Selection efficiencies and remaining number of signal and background events after each cut in the $\tau\mu E_T^{miss}$ final state. The charged Higgs mass is set to 175 GeV and $\tan\beta=100$. Numbers in parentheses are relative efficiencies in percent with respect to the previous cut. Branching ratios have been taken into account in transition from the second to third row.

In order to have an estimation of the signal significance, all selection cuts are applied sequentially and their relative efficiencies with respect to the previous cut and the number of events which survive after each cut are listed in special tables. Table II lists selection cuts efficiencies and the number of signal and background events remaining after each cut. Using the number of signal and background events remaining after all selection cuts (the last row of Tab. II) the signal significance is calculated using Eq. 9 which is based on the fact that the number of background events is large enough to be considered as a Gaussian distribution.

$$\text{Signal Significance} = \frac{N_S}{\sqrt{N_B}} \quad (9)$$

Using Eq. 9 the signal significance with $m_{(H^\pm)} = 175\text{ GeV}$ and $\tan\beta=100$ is estimated to be $\sim 2.9\sigma$ with a data corresponding to 30 fb^{-1} integrated luminosity. This is naively an evidence for the signal. At high luminosity run of LHC when 300 fb^{-1} data is collected the signal significance turns out to be 9σ with $m_{(H^\pm)} = 175\text{ GeV}$ and $\tan\beta=100$. Since the signal cross section is not purely proportional to $\tan\beta^2$ (Ref. [10]), the border of 5σ contour (the point below which the signal significance is below 5σ) can not be obtained by rescaling of results. Instead the minimum $\tan\beta$ for 5σ is obtained by running PYTHIA and trying different $\tan\beta$ values. As a result a charged Higgs with a mass $m_{(H^\pm)} = 175\text{ GeV}$ is observable in the leptonic final state search if $\tan\beta > 72$ and lower $\tan\beta$ values are out of 5σ reach.

It should be mentioned that using state of the art algorithms developed by LHC experiments, the fake rate is expected to be much smaller than what is observed in this analysis. Since W +jets background is the main background and is a source of τ fake rate, it is expected that this background would be under control in an LHC experiment analysis and lower $\tan\beta$ values would be in the 5σ reach.

B. Heavy Charged Higgs Search, Hadronic Final State

The heavy charged Higgs has been studied with this channel in hadronic final state in Ref. [9]. In this analysis the intention is a closer look to this final state including main background samples and a τ -id as close to what is in use by LHC experiments as possible. The event selection is described in the following. An event must satisfy all the following requirements to be selected:

- There should be three jets satisfying Eq. 10. The transverse energy threshold is set to the softer value of 30 GeV compared to the case of leptonic final state in order to avoid unwanted decrease of signal statistics when three jets are required.

$$E_T^{\text{jet}} > 30\text{ GeV}, \quad |\eta| < 2.5. \quad (10)$$

There has to be exactly three jets in the event and all pairs of jets are required to be well separated by Eq. 11.

$$\Delta R_{(j,j)} > 0.4, \quad \Delta R_{(\tau,j)} > 0.4. \quad (11)$$

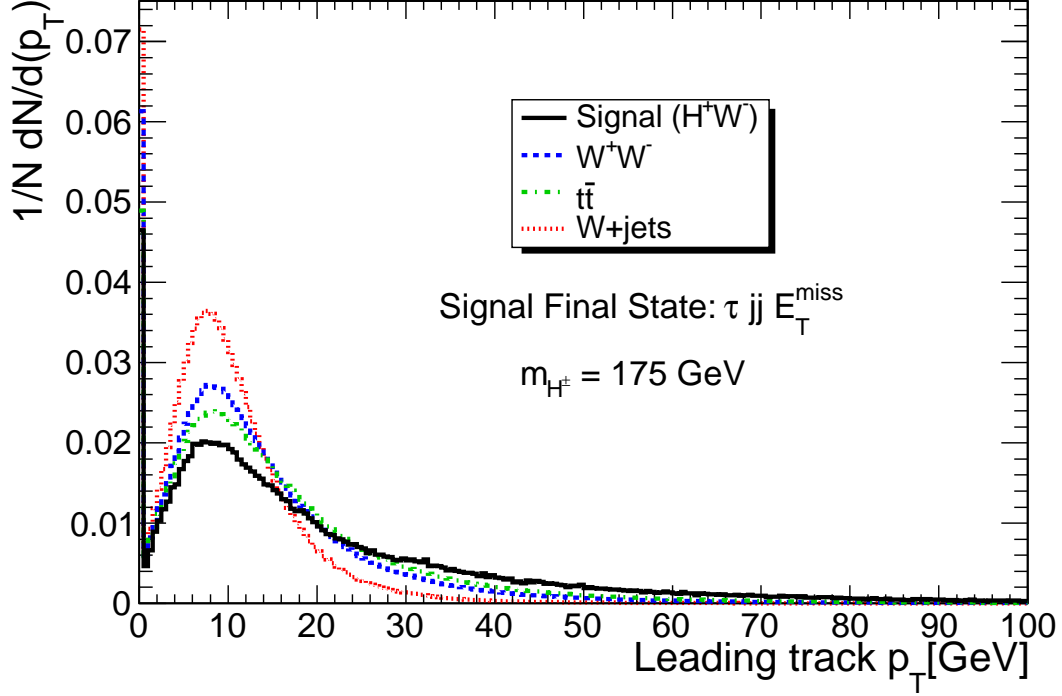


FIG. 8: Transverse momentum distribution of the leading track in the τ jet cone.

- The τ -id algorithm is then applied on selected jets in the same way as is done in the leptonic final state search. Exactly one of jets must pass the τ -id algorithm. Figures 8, 9, 10 show the distributions of related variables used in the τ -id algorithm.
- The other two jets remaining in the event are used for W mass reconstruction and their invariant mass is calculated as the W boson mass. The reconstructed W mass should fall within the W mass window defined in Eq. 12.

$$|m_{(j,j)} - 75| < 20 \text{ GeV} . \quad (12)$$

The adopted central value for the W invariant mass is a slightly lower than the current values. This is because the reconstructed jet energy may be different from the true value and the calculated invariant mass turns out to be slightly lower than the nominal value of 80 GeV. This is a known issue which is resolved by jet energy correction algorithms developed in LHC experiments. Figure 11 shows the invariant mass of the two jets as the W boson mass candidate.

- The missing transverse energy is also used to discriminate between the signal and background. Fig. 12 shows the distribution of E_T^{miss} in signal and background events. As seen from Fig. 12 the E_T^{miss} distribution is much harder in signal events. Since the charged Higgs (H^+) is spinless, in its decay, it produces a left-handed ν_τ and a left-handed τ^+ . In the subsequent τ^+ decay, the right-handed $\bar{\nu}_\tau$ is kicked back to conserve the mother τ^+ helicity. Therefore the two neutrinos preferably fly in the same direction producing a large amount of E_T^{miss} in the signal event. The following requirement on E_T^{miss} threshold is applied:

$$E_T^{miss} > 50 \text{ GeV} . \quad (13)$$

- A study of azimuthal angle between the τ jet and E_T^{miss} shows that background events tend to produce the neutrino back-to-back with respect to the τ jet. The main source of E_T^{miss} in background events is the neutrino from the W boson decay when $W \rightarrow \tau\nu$ occurs. This decay prefers the τ jet and the neutrino to fly back-to-back in the W rest frame. The change of the angle between the decay products when transferred to the lab frame is less than the case of charged Higgs boson and thus majority of background events tend to produce high values of $\Delta\phi_{(\tau, E_T^{miss})}$. Since the charged Higgs is heavy ($\sim 2 \times m_W$), when it is produced, it acquires a higher p_T compared to W boson (e.g. from W^+W^- events) as shown in Fig. 13 and thus gives a higher boost to the decay products leading to smaller angles in the lab frame. The difference is, of course, more obvious for heavier charged Higgs bosons. This feature results in lower $\Delta\phi_{(\tau, E_T^{miss})}$ in signal events as shown in Fig. 14 and is used by applying the requirement as in Eq. 14.

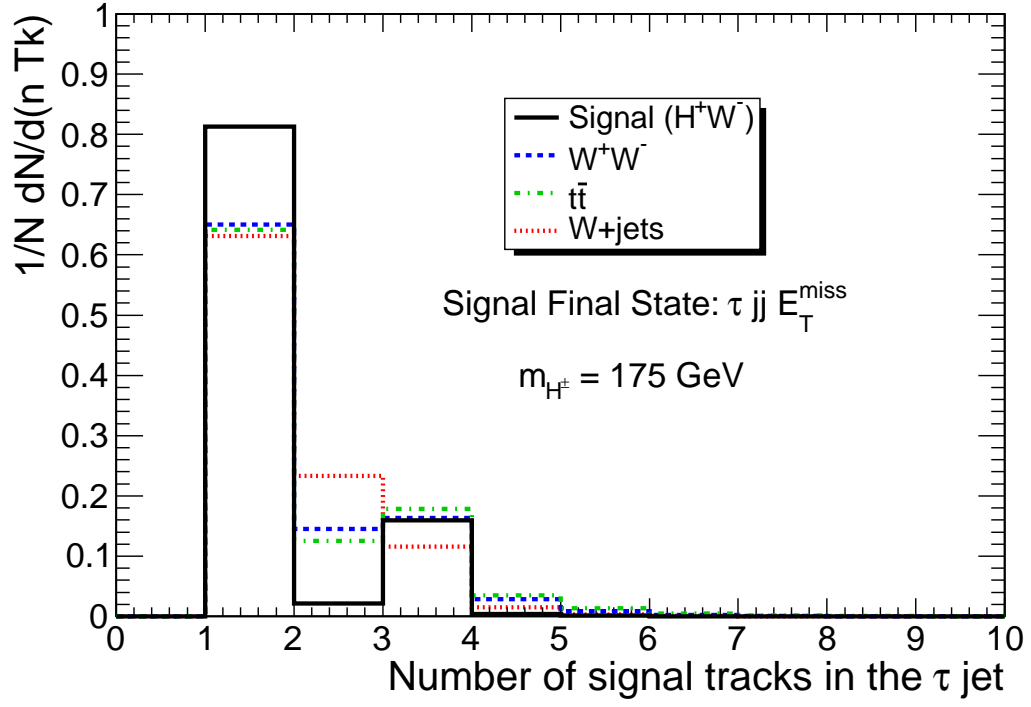


FIG. 9: Number of tracks in the signal cone around the leading track of the τ jet.

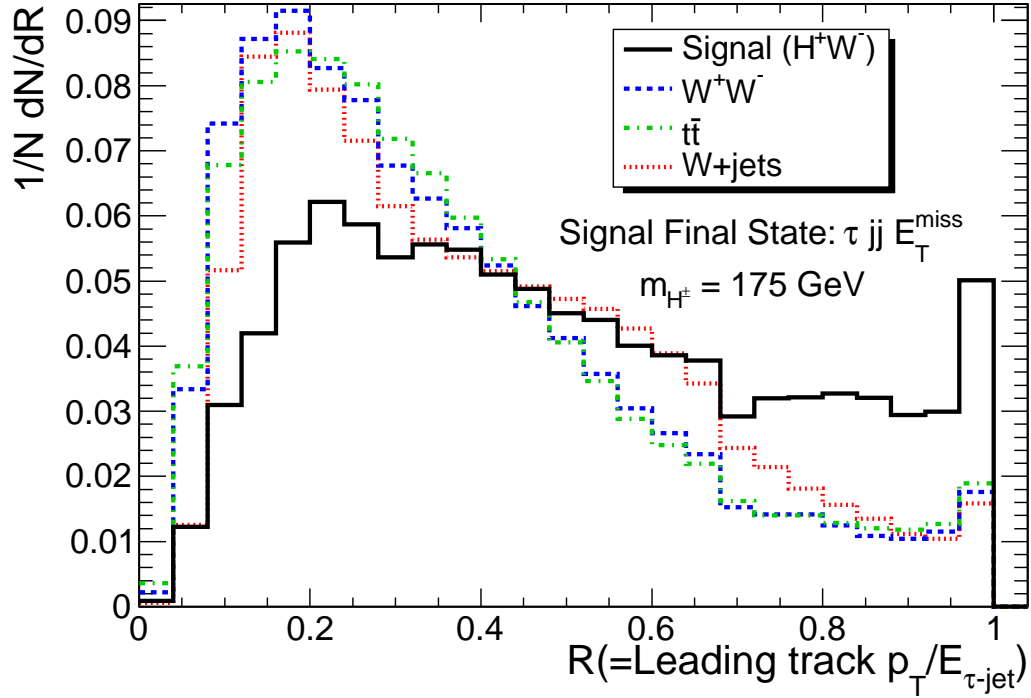


FIG. 10: Distribution of the leading track p_T divided by the τ jet energy.

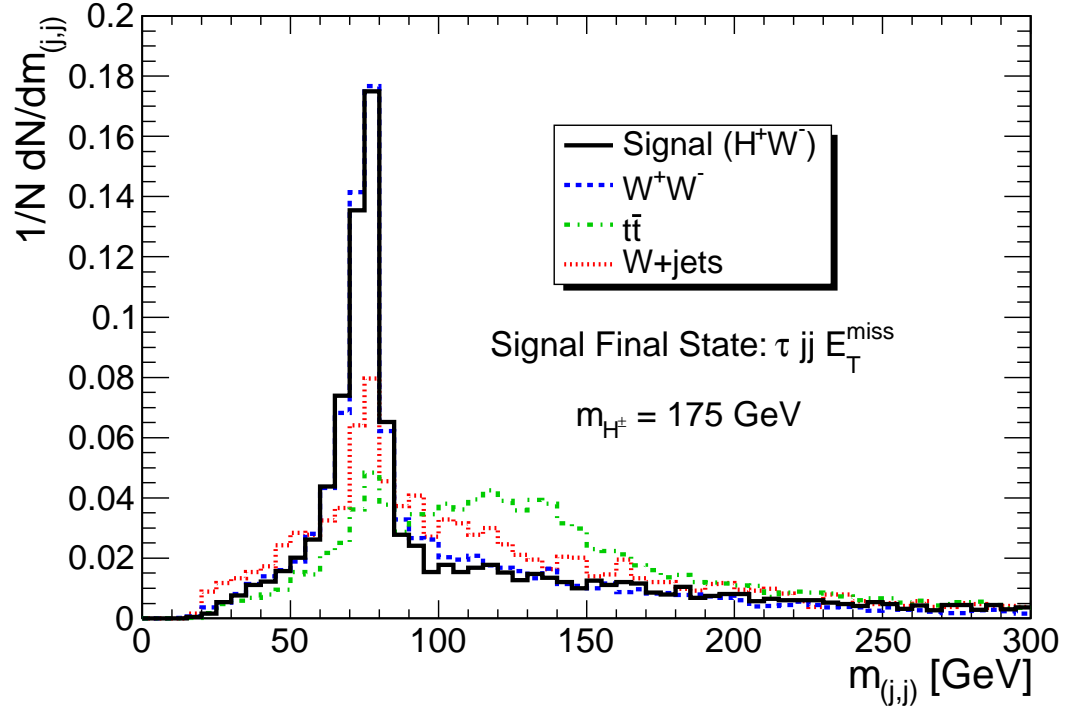


FIG. 11: Invariant mass of the two jets as the candidate pair from W boson decay.

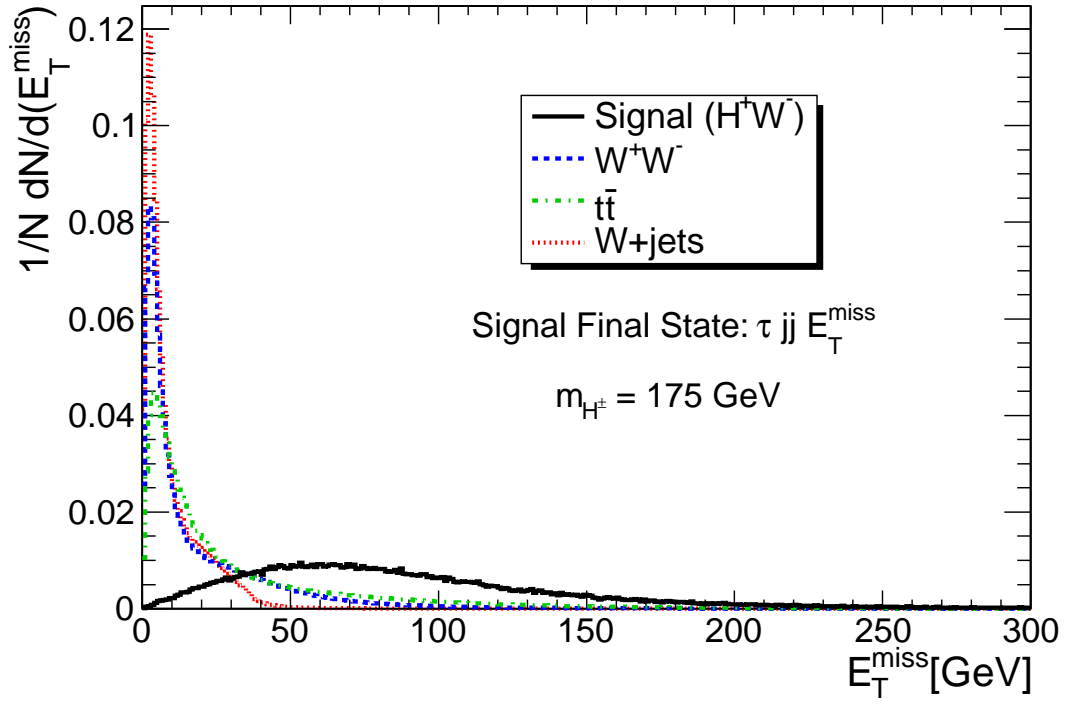


FIG. 12: Missing transverse energy distribution in signal and background events in the $\tau \, jj \, E_T^{\text{miss}}$ final state search.

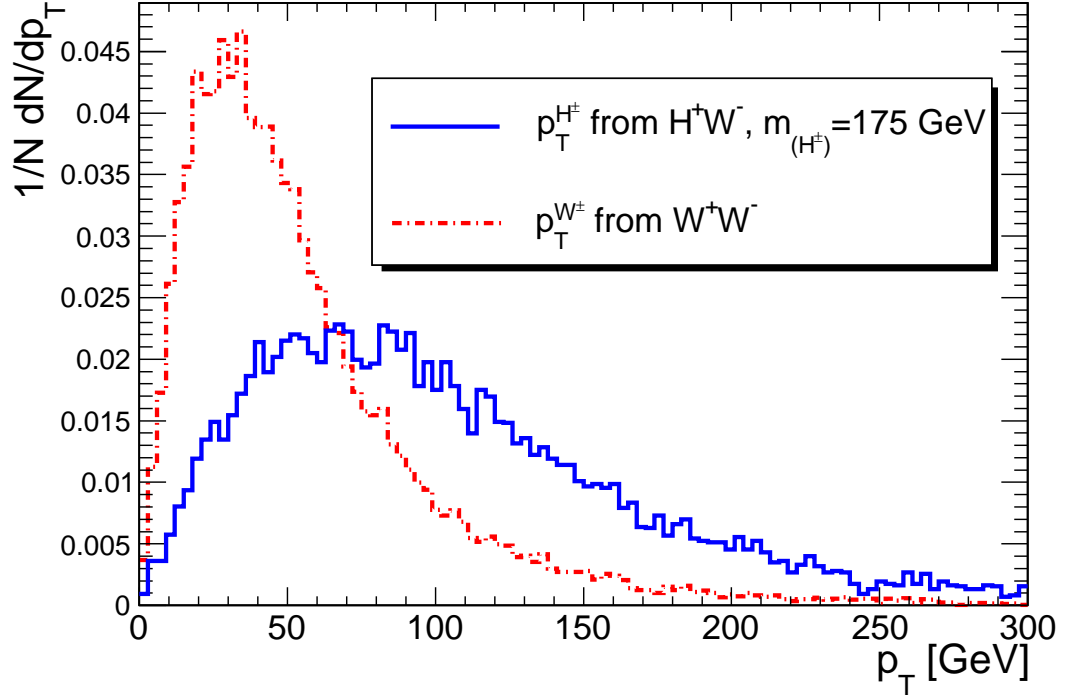


FIG. 13: The transverse momentum distribution of charged Higgs with $m_{(H^\pm)} = 175$ GeV in $H^\pm W^\mp$ events and W boson in W^+W^- .

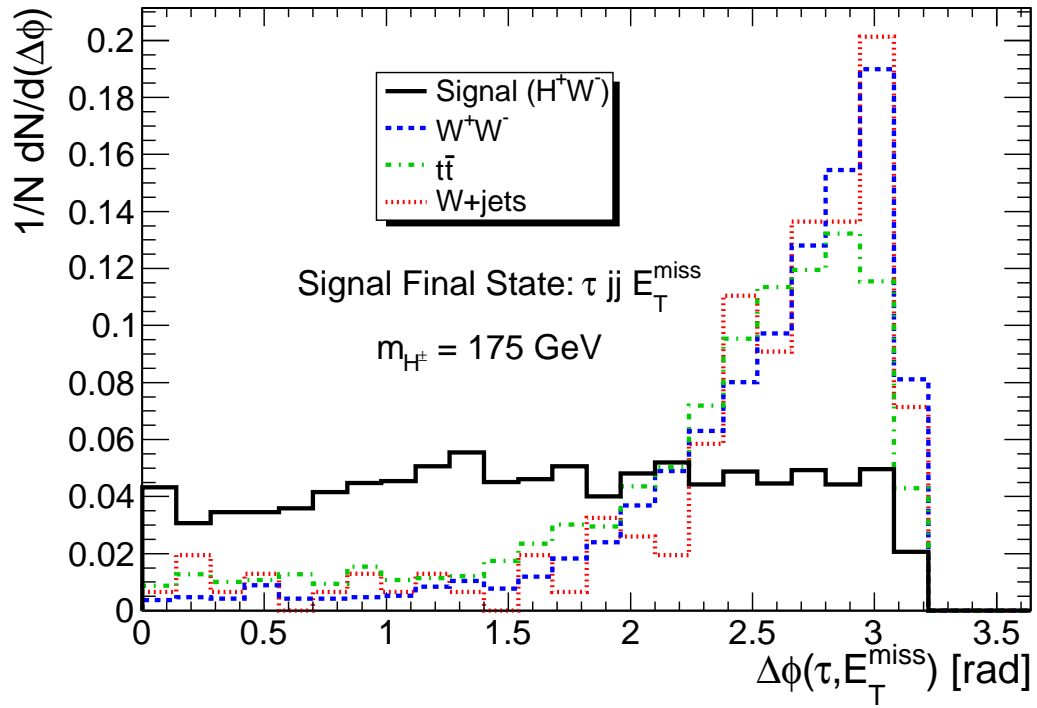


FIG. 14: The azimuthal angle between the τ jet and E_T^{miss} in the $\tau jj E_T^{miss}$ final state search.

Process	$H^\pm W^\mp$	$W^+ W^-$	$t\bar{t}$	W+jets
Total cross section [pb]	1.18	115.5	879	187100
Number of events at 30 fb^{-1}	23629	2154302	16393214	4.4×10^9
N Jets = 3	6523(27.6%)	403831(18.7%)	3.2e+06(19.5%)	4e+07(0.9%)
leading track $p_T > 20\text{ GeV}$	5086(78%)	195290(48.3%)	2e+06(59.5%)	1.8e+07(45.5%)
Isolation	3179(62.5%)	33839(17.3%)	244890(12.9%)	2.4e+06(13.2%)
R > 0.2	1890(59.4%)	12640(37.3%)	95490(39%)	752987(31.6%)
1- or 3-prong decay	1848(97.8%)	10104(80%)	83556(87.5%)	498813(66.2%)
Exactly one τ jet	1841(99.6%)	10037(99.3%)	83015(99.3%)	497493(99.7%)
W mass window	975(53%)	5543(55.2%)	18803(22.6%)	169107(34%)
$E_T^{miss} > 50\text{ GeV}$	732(75.1%)	2070(37.3%)	12205(65%)	22587(13.3%)
$\Delta\phi_{(\tau, E_T^{miss})}$	573(78.2%)	697(33.7%)	5615(46%)	7773(34.4%)
Total efficiency	2.43%	0.032%	0.034%	0.000177%
Expected events at 30 fb^{-1}	573	697	5615	7773

TABLE III: Selection efficiencies and remaining number of signal and background events after each cut in the $\tau jj E_T^{miss}$ final state search. The charged Higgs mass is set to 175 GeV and $\tan\beta = 100$. Numbers in parentheses are relative efficiencies in percent with respect to the previous cut. Branching ratios have been taken into account in transition from the second to third row.

$$\Delta\phi_{(\tau, E_T^{miss})} < 2.5. \quad (14)$$

With the above selection cuts, Tab. III lists the selection efficiencies and the remaining number of events after each cut. Using the number of events as in Tab. III the signal significance is estimated to be 4.8σ for $m_{(H^\pm)} = 175\text{ GeV}$ and $\tan\beta = 100$ at 30 fb^{-1} integrated luminosity. At high luminosity run of LHC, the signal significance could increase to 15σ . The $\tan\beta$ value for which the signal significance at high luminosity is 5σ is estimated to be $\tan\beta \simeq 55$.

C. Light Charged Higgs Search, Leptonic Final State

In the following, the contribution of $H^\pm W^\mp$ to the low mass region search in the two categories of leptonic and hadronic final states is estimated. In other words the additional contribution solely from $H^\pm W^\mp$ to $t\bar{t} \rightarrow H^\pm W^\mp b\bar{b}$ which is the main signal in the low mass region is estimated. Having passed a common set of selection cuts, $H^\pm W^\mp$ signal should appear as an excess of events over what is observed from $t\bar{t} \rightarrow H^\pm W^\mp b\bar{b}$ events. What is expected is that the final number of $t\bar{t} \rightarrow H^\pm W^\mp b\bar{b}$ events should be dominant in the signal region due to the large total cross section of this process. One may imagine that a leptonic final state search for events with one jet (the τ jet) in the final state may produce an $H^\pm W^\mp$ dominant sample. This is not the case because $t\bar{t} \rightarrow H^\pm W^\mp b\bar{b}$ events have sizable contribution even to the one-jet bin due to their large cross section at the LHC (Fig. 15). To verify this fact the same set of selection cuts as what was used in the heavy charged Higgs leptonic final state search is applied on $H^\pm W^\mp$ and $t\bar{t} \rightarrow H^\pm W^\mp b\bar{b}$ events. The chosen parameters for the simulation are $m_{(H^\pm)} = 150\text{ GeV}$ and $\tan\beta = 100$. Table IV lists the selection efficiencies and the remaining number of events after each cut. Therefore as seen from Tab. IV, although the selection efficiency of the $H^\pm W^\mp$ process is roughly 7 times larger they would appear as only 3% excess over $t\bar{t} \rightarrow H^\pm W^\mp b\bar{b}$ events in the leptonic final state search.

D. Light Charged Higgs Search, Hadronic Final State

The contribution of $H^\pm W^\mp$ to the light charged Higgs search can also be estimated by applying the same selection cuts as was done in the heavy charged Higgs hadronic final state analysis. These cuts are applied on both $H^\pm W^\mp$ and $t\bar{t} \rightarrow H^\pm W^\mp b\bar{b}$ events for comparison. Table V shows the selection efficiencies and the remaining number of events after each cut. As seen from Tab. V, $H^\pm W^\mp$ events appear as a $\sim 1.5\%$ excess over $t\bar{t} \rightarrow H^\pm W^\mp b\bar{b}$ events in the hadronic final state. Therefore in both categories of leptonic and hadronic searches, in the low mass region, the dominant production process is $t\bar{t} \rightarrow H^\pm W^\mp b\bar{b}$.

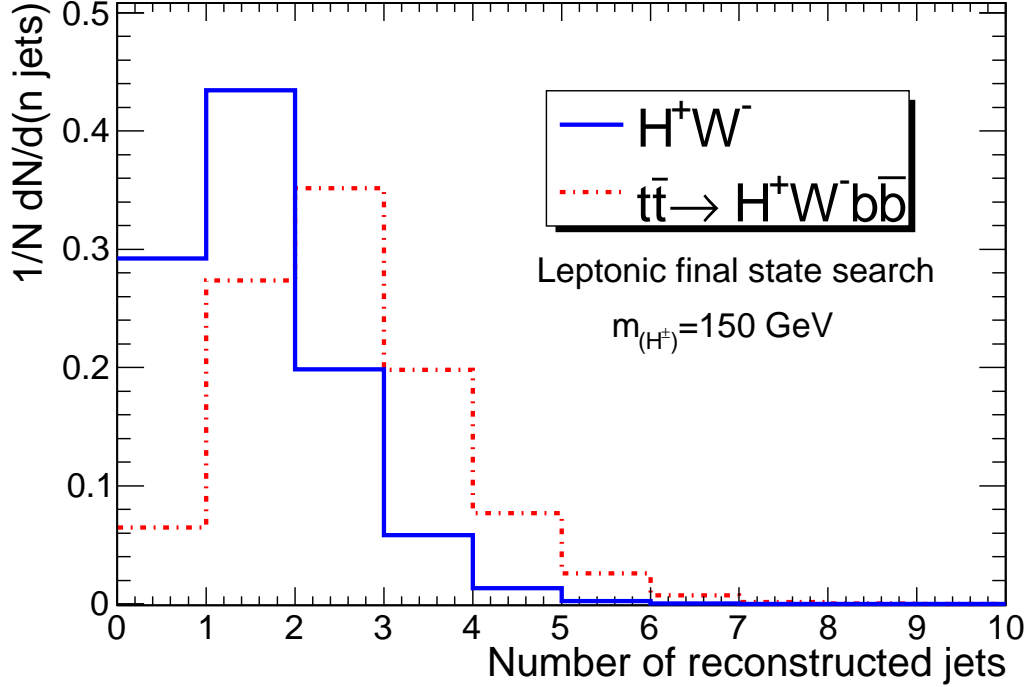


FIG. 15: Jet Multiplicity in $H^\pm W^\mp$ and $t\bar{t} \rightarrow H^\pm W^\mp b\bar{b}$ events in the leptonic final state search with $m_{(H^\pm)} = 150$ GeV.

Process	$H^\pm W^\mp$	$t\bar{t} \rightarrow H^\pm W^\mp b\bar{b}$
Total cross section [pb]	1.47	878.7
Number of events at 30 fb^{-1}	4601	963487
N Muons = 1	2114(45.9%)	381888(39.6%)
N Jets = 1	923(43.7%)	98411(26%)
leading track $p_T > 20$ GeV	499(54%)	29020(29.5%)
Isolation	395(79.2%)	12728(43.8%)
R > 0.2	347(87.7%)	10743(84.4%)
1- or 3-prong decay	341(98.4%)	10463(97.4%)
Opposite charge	341(99.9%)	10251.5(98%)
$E_T^{miss} > 50$ GeV	226(66.4%)	6513(63.5%)
Total efficiency	4.9%	0.67%
Expected events at 30 fb^{-1}	226	6513

TABLE IV: Selection efficiencies and remaining number of $H^\pm W^\mp$ and $t\bar{t} \rightarrow H^\pm W^\mp b\bar{b}$ events after each cut in the $\tau\mu E_T^{miss}$ final state. The charged Higgs mass is set to 150 GeV and $\tan\beta = 100$. Numbers in parentheses are relative efficiencies in percent with respect to the previous cut. Branching ratios have been taken into account in transition from the second to third row.

VI. 5σ AND 3σ CONTOURS

In order to obtain 5σ and 3σ contours, two more points in the parameter space are studied. They are $m_{(H^\pm)} = 190, 200$ GeV with $\tan\beta = 100$. Table VI shows the cross sections and efficiencies related to these points. It should be noted that the branching ratio of charged Higgs decay to $\tau\nu$ decreases with increasing charged Higgs mass. Using HDECAY, the following values are obtained and used in the analysis: $\text{BR}(H^\pm \rightarrow \tau\nu) = 0.9$ for $m_{(H^\pm)} = 190$ GeV and $\text{BR}(H^\pm \rightarrow \tau\nu) = 0.83$ for $m_{(H^\pm)} = 200$ GeV. It should be noted that although the signal significance stated by Eq. 9

Process	$H^\pm W^\mp$	$t\bar{t} \rightarrow H^\pm W^\mp b\bar{b}$
Total cross section [pb]	1.47	878.7
Number of events at 30 fb^{-1}	29435	6163817
N Jets = 3	7796(26.5%)	1.9e+06(30.3%)
leading track $p_T > 20\text{ GeV}$	5928(76%)	1.3e+06(67.4%)
Isolation	3579(60.4%)	507282(40.2%)
R > 0.2	2168(60.6%)	281563(55.5%)
1- or 3-prong decay	2113(97.4%)	271331(96.4%)
Exactly one τ jet	2106(99.7%)	270715(99.8%)
W mass window	1130(53.7%)	77171(28.5%)
$E_T^{miss} > 50\text{ GeV}$	785(69.4%)	48448(62.8%)
$\Delta\phi_{(\tau, E_T^{miss})}$	551(70.2%)	34641(71.5%)
Total efficiency	1.87%	0.56%
Expected events at 30 fb^{-1}	551	34641

TABLE V: Selection efficiencies and remaining number of $H^\pm W^\mp$ and $t\bar{t} \rightarrow H^\pm W^\mp b\bar{b}$ events after each cut in the $\tau jj E_T^{miss}$ final state search. The charged Higgs mass is set to 150 GeV and $\tan\beta = 100$. Numbers in parentheses are relative efficiencies in percent with respect to the previous cut. Branching ratios have been taken into account in transition from the second to third row.

$m_{(H^\pm)}$	Total cross section	eff _{lep.}	$N_S^{lep.}$	eff _{had.}	$N_S^{had.}$
190 GeV	1043 fb	5.88%	176	2.74%	524
200 GeV	954.4 fb	6.04%	152	2.89%	465

TABLE VI: Cross sections and efficiencies of leptonic and hadronic final state searches for $m_{(H^\pm)} = 190, 200\text{ GeV}$ and $\tan\beta = 100$. eff_{lep.}(eff_{had.}) is the signal efficiency in leptonic (hadronic) final state search and $N_S^{lep.}$ ($N_S^{had.}$) is the number of signal events which pass all the selection cuts at 30 fb^{-1} .

grows like \sqrt{L} where L is the integrated luminosity, in reality this assumption may not be the case especially when systematic uncertainties are introduced in the signal significance calculation. The estimation of such effects is beyond the scope of this work and needs a full simulation at the presence of detector effects. In this work discovery potential of the studied signal is presented. Figures 16 and 17 show the estimated 5σ discovery and 3σ evidence contours if a leptonic final state search is carried out. Accordingly Figs. 18 and 19 show the 5σ discovery and 3σ evidence contours with the hadronic final state search.

VII. CONCLUSIONS

The associated production of charged Higgs and W boson were studied in the framework of MSSM. The signal observability in the leptonic final state search, i.e. $H^\pm W^\mp \rightarrow \ell \tau E_T^{miss}$ with $\ell = e$ or μ and also the hadronic final state search, i.e. $H^\pm W^\mp \rightarrow \tau jj E_T^{miss}$ was investigated. The analysis is suitable for a high luminosity study at an integrated luminosity of 300 fb^{-1} . Results indicate that in the low mass region ($m_{(H^\pm)} < 175\text{ GeV}$) this signal only appears as 3% (1.5%) excess over what is observed from the dominant $t\bar{t} \rightarrow H^\pm W^\mp b\bar{b}$ process in the leptonic (hadronic) final state search. In the high mass region at an integrated luminosity of 300 fb^{-1} , a charged Higgs with $m_{(H^\pm)} = 175\text{ GeV}$, in the leptonic final state search, is in the 5σ discovery reach if $\tan\beta > 72$. The 3σ contour starts from $\tan\beta > 56$. The hadronic final state search leads to 5σ signal for $\tan\beta > 55$ with $m_{(H^\pm)} = 175$. The 3σ evidence in the hadronic final state search starts from $\tan\beta > 43$. Although high $\tan\beta$ values are accessible with this channel, adding this signal to the current searches, especially in the high mass search, may provide broader regions in the parameter space than what is currently available. This requires a full simulation at the presence of detector effects

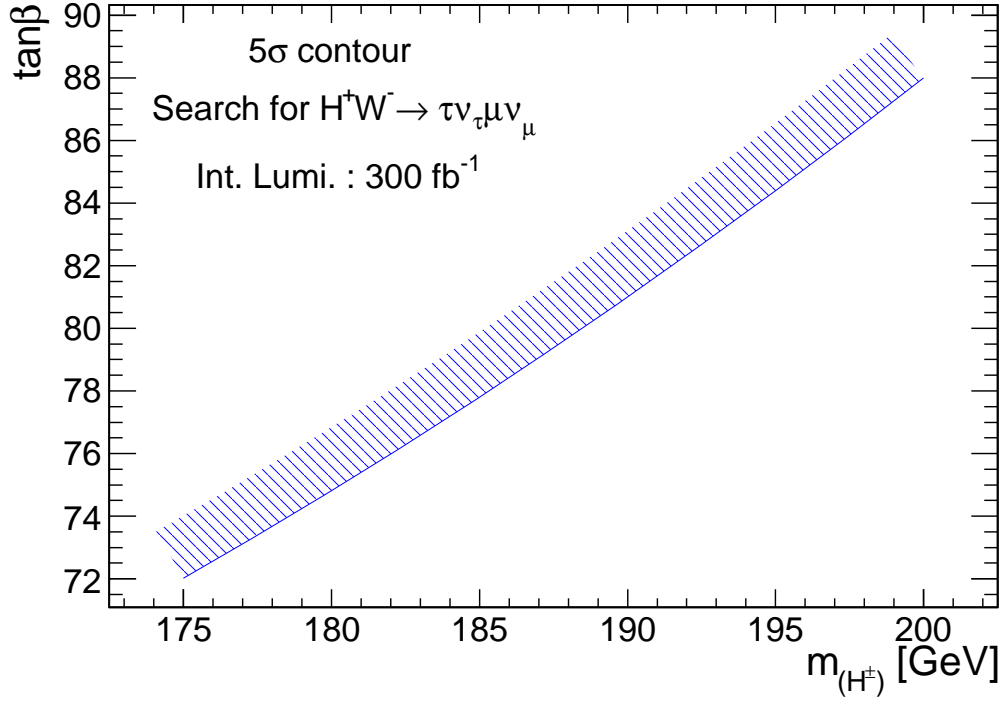


FIG. 16: The 5σ discovery contour obtained with the leptonic final state search. The integrated luminosity is set to 300 fb^{-1} .

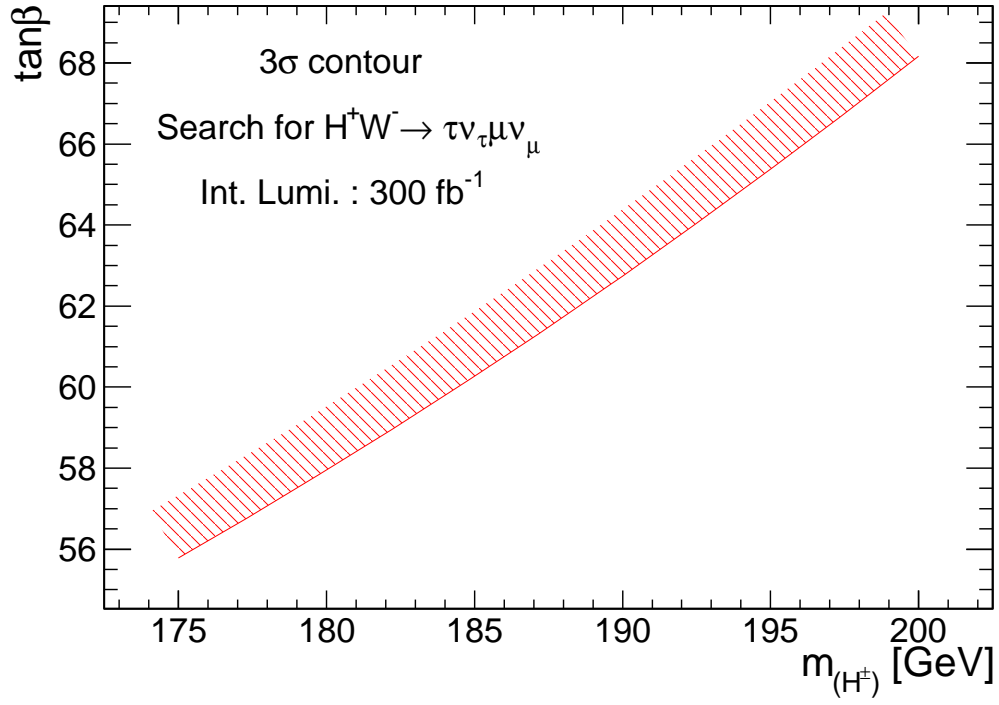


FIG. 17: The 3σ evidence contour obtained with the leptonic final state search. The integrated luminosity is set to 300 fb^{-1} .

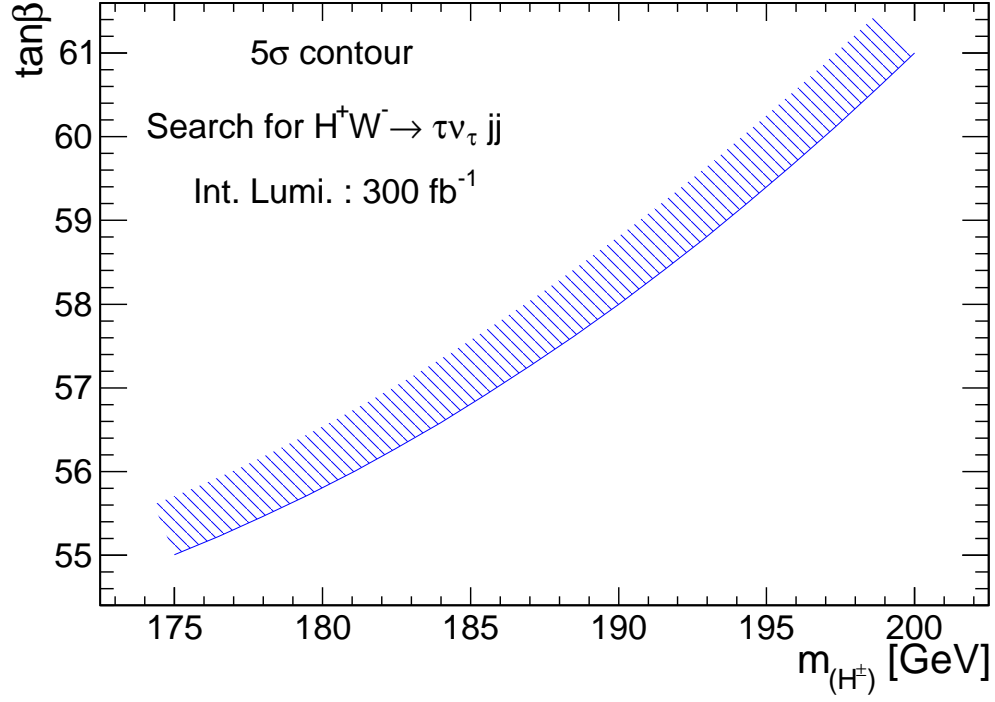


FIG. 18: The 5 σ discovery contour obtained with the hadronic final state search. The integrated luminosity is set to 300 fb $^{-1}$.

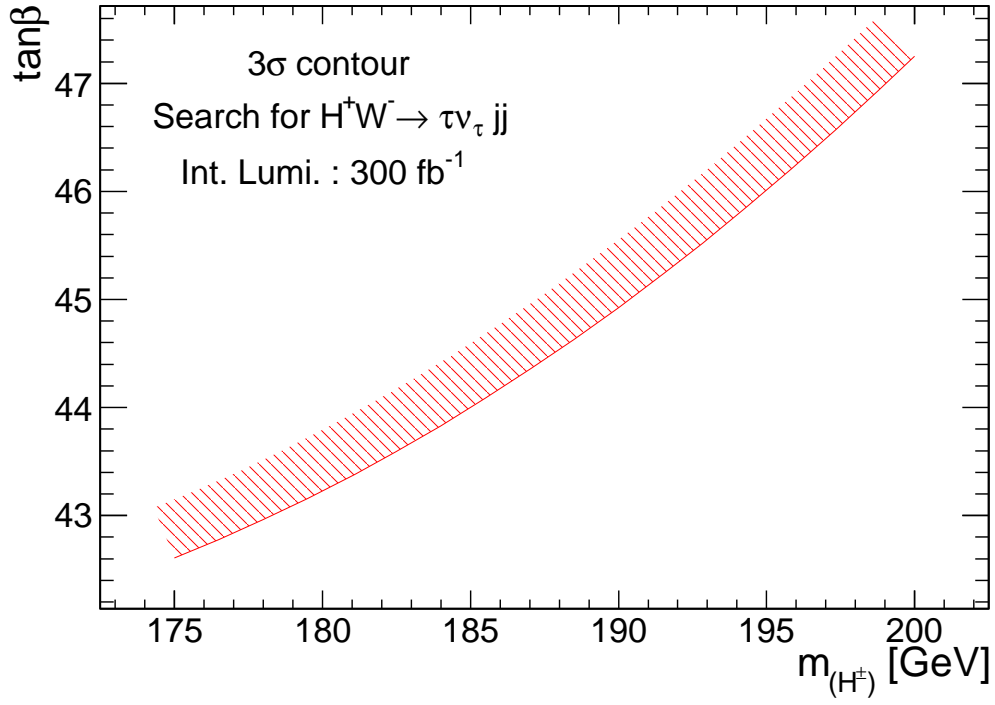


FIG. 19: The 3 σ evidence contour obtained with the hadronic final state search. The integrated luminosity is set to 300 fb $^{-1}$.

which can be done by CMS and ATLAS collaborations as a follow up of this work.

-
- [1] S. P. Martin, hep-ph/9709356
 - [2] M. Baarmand, M. Hashemi, A. Nikitenko, J. Phys. G: Nucl. Part. Phys. 32 (2006) N21
 - [3] R. Kinnunen, CMS-NOTE-2006-100
 - [4] S. Lowette, J. D'Hondt, P. Vanlaer, CMS-NOTE-2006-109
 - [5] ATLAS Collaboration, CERN-OPEN-2008-020 [hep-ex/09010512]
 - [6] ATLAS Collaboration, ATL-PHYS-PUB-2010-006
 - [7] T. Plehn, Phys. Rev. D 67 (2003) 014018
 - [8] E. L. Berger, T. Han, J. Jiang, T. Plehn, hep-ph/0312286
 - [9] D. Eriksson, S. Hesselbach, J. Rathsmann, J. of Phys.: Conf. Ser. 110 (2008) 072008
 - [10] D. Eriksson, S. Hesselbach, J. Rathsmann, hep-ph/0612198
 - [11] D. A. Dicus, J. L. Hewett, C. Kao, T. G. Rizzo, Phys. Rev. D 40 (1989) 787
 - [12] A. A. Barrientos Bendezu, B. A. Kniehl, Phys. Rev. D 59 (1998) 015009
 - [13] D. Eriksson, hep-ph/09020510
 - [14] T. Sjstrand et al, JHEP05(2006)026
 - [15] S. Jadach, Z. Was, R. Decker, J.H. Kühn, Comp. Phys. Comm. 76(1993)361
 - [16] M. Jezabek, Z. Was, S. Jadach, J.H. Kühn, Comp. Phys. Comm. 70(1992)69
 - [17] S. Jadach, J.H. Kühn, Z. Was, Comp. Phys. Comm. 64(1990)275
 - [18] <http://projects.hepforge.org/lhapdf/>
 - [19] <http://mcfm.fnal.gov/>
 - [20] <http://pdg.lbl.gov/2009/listings/rpp2009-list-w-boson.pdf>
 - [21] A. Djouadi, J. Kalinowski, M. Spira, Comp. Phys. Comm. 108 (1998) 56 [hep-ph/9704448]
 - [22] CMS Collaboration, CMS Physics, Technical Design Report, volume I, CERN-LHCC-2006-001, section 12.1.2